Neutrino signal from Cygnus region of the Milky Way

Andrii Neronov,[1,2] Dmitri Semikoz,[1] and Denys Savchenko[1,3,4]

[1]*Université Paris Cité, CNRS, Astroparticule et Cosmologie, F-75013 Paris, France*
[2]*Laboratory of Astrophysics, École Polytechnique Fédérale de Lausanne, CH-1015 Lausanne, Switzerland*
[3]*Bogolyubov Institute for Theoretical Physics of the NAS of Ukraine, 03143 Kyiv, Ukraine*
[4]*Kyiv Academic University, 03142 Kyiv, Ukraine*

(Received 29 January 2024; accepted 14 July 2024; published 14 August 2024)

Interactions of cosmic-ray protons and nuclei in their sources and in the interstellar medium produce "hadronic" γ-ray emission. Gamma rays can also be of "leptonic" origin, i.e., originating from high-energy electrons accelerated together with protons. It is difficult to distinguish between hadronic and leptonic emission mechanisms based on γ-ray data alone. This can be done via detection of neutrinos, because only hadronic processes lead to neutrino production. We use the publicly available 10 yr IceCube neutrino telescope dataset to demonstrate the hadronic nature of high-energy emission from the direction of the Cygnus region of the Milky Way. We find a 3σ excess of neutrino events from an extended Cygnus Cocoon, with the flux comparable to the flux of γ rays in the multi-TeV energy range seen by HAWC and LHAASO telescopes.

DOI: 10.1103/PhysRevD.110.043024

I. INTRODUCTION

The bulk of cosmic rays penetrating Earth's atmosphere is composed of high-energy protons and atomic nuclei coming from yet uncertain astronomical sources in the Milky Way Galaxy. Astronomical objects produced in supernova explosions and superbubbles of star formation are considered as candidate cosmic-ray source classes [1]. Firm identification of the cosmic-ray sources can be done via observations of multimessenger neutrino and γ rays produced in cosmic-ray interactions.

IceCube telescope has found evidence for the neutrino signal from the Milky Way [2–5], but has not yet located individual cosmic-ray sources in the Galaxy. Contrary to the neutrino signal, high-energy γ-ray flux from cosmic-ray proton and nuclei interactions has perhaps been already detected from multiple known Galactic sources. However, γ rays can be produced not only in interactions of the cosmic-ray protons and nuclei, but also by high-energy electrons. The only way to unambiguously distinguish hadronic (proton or nuclei powered) and leptonic (electron powered) emission is to detect the neutrino flux accompanying the γ-ray flux from proton and nuclei interactions.

Previous γ-ray based estimate of neutrino flux from the Galactic sources provides a prediction that the most promising candidate neutrino source in the Northern Hemisphere is the Cygnus region of the Milky Way disk, detectable at more than 3σ significance level in decade-scale exposure [6]. This active star formation region [7] hosts multiple massive star associations, supernova remnants, pulsar wind nebulae [8], and a hard γ-ray spectrum diffuse emission region Cygnus Cocoon [9–13].

The γ-ray data [9,12–14] indicate that the high-energy source in the Cygnus region has complex morphology. Fermi/LAT [9], ARGO [12], HAWC [13], and LHAASO [14] telescopes all find that the signal is not from a point source. Modeling of the γ-ray signal morphology reveals a more compact source (TeV J2032 + 4130, first detected by the HEGRA telescope [10]) close to the location of the pulsar PSR J2032 + 4127 and a more extended source associated with diffuse emission from a "Cocoon" with radius about 2° (first discovered by Fermi/LAT [9]). The overall γ-ray flux from the region is dominated by the Cocoon [13]. This source, detected up to PeV energy range by LHAASO [14], seems to have energy-dependent morphology: the position of the higher-energy source seen by the KM2A detector of LHAASO is shifted with respect to that of the lower-energy WCDA detector source, while a doublet of highest energy PeV photons is further displaced with respect to the position of the KM2A source centroid [14], see Fig. 2. The spectrum of the γ-ray source is softening with energy. LHAASO WCDA data are consistent with a power-law spectral model $dN/dE \propto E^{\Gamma}$ with the slope $\Gamma = -2.63 \pm 0.08$, while the KM2A source is described by a power law with the slope $\Gamma = -2.99 \pm 0.07$ [14]. Even though it is not possible to unambiguously determine the origin of the γ-ray emission, HAWC [13] and LHAASO [14] data interpretation suggest that the bulk of

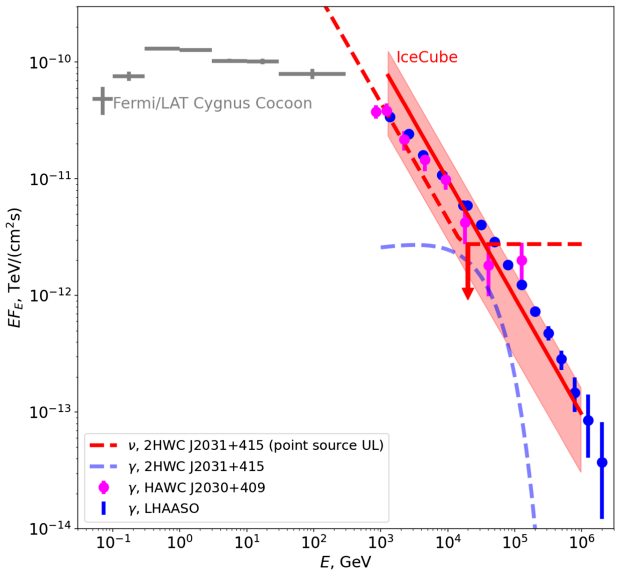

FIG. 1. Spectrum of extended multimessenger signal from the Cygnus region. Red solid line shows the best-fit all-flavor neutrino spectrum, red shaded region shows the 68% confidence interval of the neutrino flux level. The flux upper limits on the point source 2HWC J2031 + 415 from IceCube point source analysis for the power-law spectra with slopes $\Gamma = 2$ and $\Gamma = 3$ are shown by the red dashed lines with an arrow [15]. Bright blue data points show the measurements of the γ-ray flux from the extended Cocoon source by LHAASO [14]. Magenta data points show HAWC spectrum of the Cocoon [13]. Gray data points show the Cygnus Cocoon γ-ray spectrum from the Fermi/LAT catalog [16]. Pale blue dashed line shows a fit to γ-ray spectrum of the compact source in 2HWC J2031 + 415 from Ref. [13].

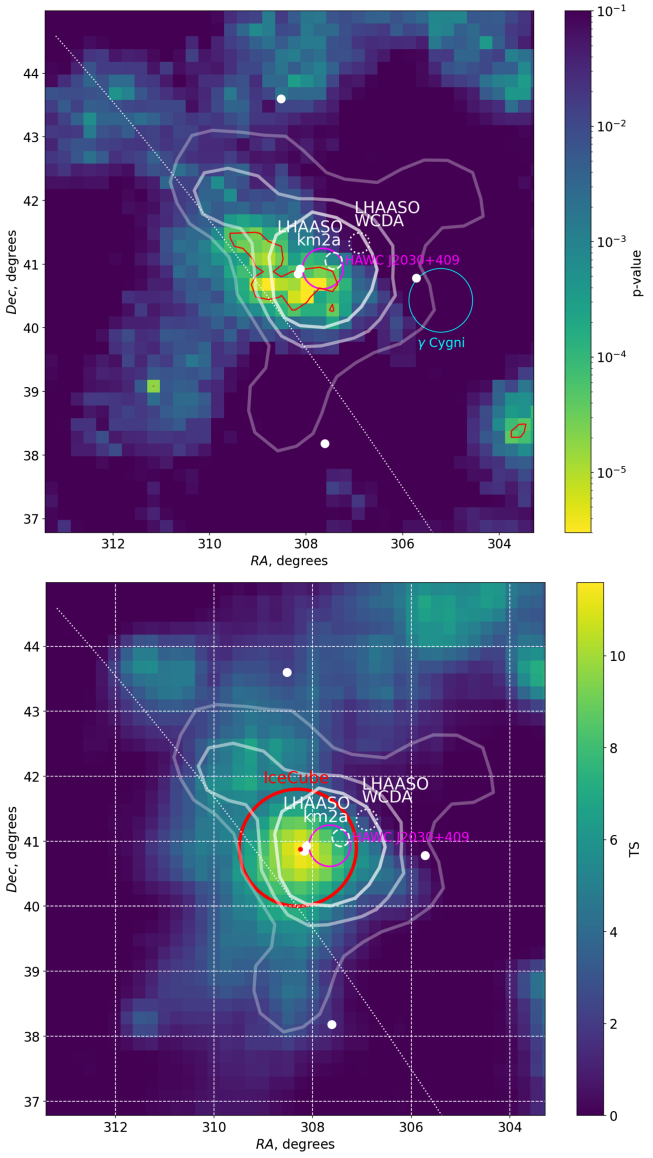

FIG. 2. Top: map of the p-values of (in)consistency of the count statistics with background-only hypothesis in the event counting analysis. Cyan circle is the position of γ Cygni supernova remnant. Magenta circle shows the uncertainty of localization of the HAWC Cocoon source. White dashed circle shows the uncertainty of position of LHAASO KM2A source, dotted circle is the position of the γ-ray source centroid measured by LHAASO WCDA. White points show the PeV energy γ rays detected by LHAASO KM2A. Contours show LHAASO significance contours of 12σ, 15σ, 18σ [14]. Inclined line marks the Galactic Plane. Red solid contour shows the $p_0 = 6 \times 10^{-4}$ p-value level. Bottom: map of the TS values of the likelihood analysis. Red dot and circle show the best fit and uncertainty of the position of the neutrino source. Other notations are the same as in the top panel.

the γ-ray flux is of hadronic origin and thus has to have the neutrino counterpart.

Search for the muon neutrino signal from the Cygnus region based on 10 yr IceCube exposure [15] has only resulted in an upper limit on a pointlike source 2HWC J2031 + 415. The limit was derived for a power-law spectrum $dN_\nu/dE_{\nu_\mu} = F_0(E_{\nu_\mu}/1\ \mathrm{TeV})^\Gamma$ with normalization F_0 in $E_{\nu_\mu} \gtrsim 1$ TeV muon neutrino energy range. This limit, reported for $\Gamma = -2$ and $\Gamma = -3$ in Ref. [15],[1] is shown in Fig. 1 as a limit on total neutrino flux.[2] The neutrino flux limit is higher than the flux of the compact γ-ray source at the position 2HWC J2031 + 415. However, it is comparable to the γ-ray flux measured by HAWC and LHAASO from the Cygnus Cocoon region, also shown in Fig. 1. Within the hadronic model of the Cocoon activity, the neutrino flux is expected to be approximately equal to the γ-ray flux. Closeness of the IceCube limit (on the point source flux) to the γ-ray source flux measurement suggests that the neutrino flux from an extended hadronic source may actually be detectable.

[1]The analysis has identified a mild excess in the direction of the source, with the best-fit power-law spectrum $\Gamma = 3.8$, but the flux estimate for such slope has not been reported.

[2]We assume total mixing of neutrino flavors, so that the total neutrino flux is 3 times higher than the muon neutrino flux.

II. NEUTRINO SOURCE IN THE DIRECTION OF THE CYGNUS REGION

We use the publicly available dataset of IceCube [15,17] to show that the neutrino signal from the Cygnus region is consistent with the expectations from the hadronic model. The main difference of our analysis from the approach of Refs. [15,17] is that we look for the flux of extended, rather than point, source in the Cygnus region. Similar to Refs. [18,19], we consider the data of the full IceCube detector, because our methods rely on homogeneity of event selection. We use two complementary approaches for the source search: the unbinned likelihood analysis and the aperture photometry.

Within the aperture photometry approach, we perform a search for a localized excess of muon neutrino events within a circle of radius R. Ideally, this excess is best seen in events of the best quality of angular reconstruction σ, but the number of best quality events with $\sigma \ll R$ is small and hence a trade-off between better localization and larger signal statistics has to be made: events with $\sigma \gtrsim R$ can be considered, but events with $\sigma \gg R$ would rather add background noise without increasing signal statistics. There exists an optimal choice of event sample with $\sigma < \sigma_{\rm cut}$ for which the signal-to-noise ratio is maximal.

We find an excess of events with the p_0 values between 6×10^{-6} and 8×10^{-5} for any possible source center location within the position uncertainty of HAWC or LHAASO source centroid. The number of the excess events in the signal region ranges between 99 and 131, depending on the source positioning, while the expected background ranges between 66 and 91 events. Top panel of Fig. 2 shows the map of the lowest p_0 values for event selections with different $\sigma_{\rm cut}$, $0.5° < \sigma_{\rm cut} < 2°$ and $0.5° < R < 2°$ centered at the position of each pixel. The red solid contour shows $p_0 = 6 \times 10^{-5}$ level, corresponding to the 4σ local significance of inconsistency of the count statistics with the expectation from the background.

The probability p_0 does not take into account the trial factor related to our choice of $R, \sigma_{\rm cut}$. To calculate this factor, we perform Monte Carlo simulations, assigning random right ascensions (RAs) to the IceCube events while leaving their declinations unchanged. We repeat the event counting analysis for each simulated dataset, finding the best $R, \sigma_{\rm cut}$ minimizing the p-value. Counting the number of occurrences of the simulated datasets with fluctuations of event statistics resulting in p-values at least as low as p_0, we estimate the posttrial probability for the observed excess to be a background fluctuation better than $p = 2.7 \times 10^{-3}$, i.e., source detection significance at $\gtrsim 3\sigma$ level for any source center position.

For the likelihood analysis, we calculate the unbinned likelihood [20]

$$\log L(N_s) = \sum_i \log\left(\frac{N_s}{N_t} S_i + \left(1 - \frac{N_s}{N_t}\right) B_i\right), \quad (1)$$

where the sum runs over the neutrino event sample, N_s, N_t are the source and total event counts, and S_i and B_i are the probability density functions (PDFs) of the signal and background for ith event.

The background on top of which the source signal is detected depends on the declination, because of the geographical location of IceCube at the South Pole. Its spectral and spatial PDF is determined by the atmospheric neutrinos [21]. Assuming that the source signal provides a minor contribution to the overall count statistics, we calculate B directly from the data, by computing the distribution of detected events in declination (Dec) and energy.

The source PDF depends on the assumed shape of the source spectrum and on the parameter(s) of the spatial model. Similar to previous IceCube source searches [15,22], we consider the power-law spectral models with fixed slope $\Gamma = -3$ consistent with the LHAASO KM2A γ-ray data. The spatial model is characterized by one parameter, R, the source extension. The point source hypothesis considered in Ref. [15] corresponds to $R = 0$. We consider two types of spatial models: a flat disk

$$\mathcal{M}(\vec{r}', R) = \begin{cases} 1/(\pi R^2), & |\vec{r}'| < R \\ 0, & |\vec{r}'| > R \end{cases} \quad (2)$$

where $\vec{r}$ is the angular displacement of event from the source center position and R is the disk radius, or a two-dimensional Gaussian of the width R,

$$\mathcal{M}(\vec{r}', R) = \frac{1}{2\pi R^2} \exp\left(-\frac{\vec{r}'^2}{2R^2}\right). \quad (3)$$

Some of the lower-quality IceCube events can have insufficient precision of angular reconstruction σ, that is comparable or larger than the source size we are interested in ($\sim 2°$). We exclude such events from our analysis by imposing a quality cut $\sigma < 1°$. We have verified that such a cut does not degrade the outcomes of the analysis, checking that exclusion of such low-quality events does not degrade the test statistic (TS) value for the sources for which an evidence of the signal has been previously reported by IceCube Collaboration [18,23,24]. We assume that the point spread function for the selected events with good quality of reconstruction of the angular direction is well described by a two-dimensional circularly symmetric Gaussian. To calculate S we convolve the spatial models of the source with two-dimensional Gaussian kernel $G_\sigma(\vec{r}, \vec{r}')$ of the width equal to the angular error σ,

$$S(\vec{r}) = \int \mathcal{M}(\vec{r}') G(\vec{r}, \vec{r}') d^2\vec{r}'. \quad (4)$$

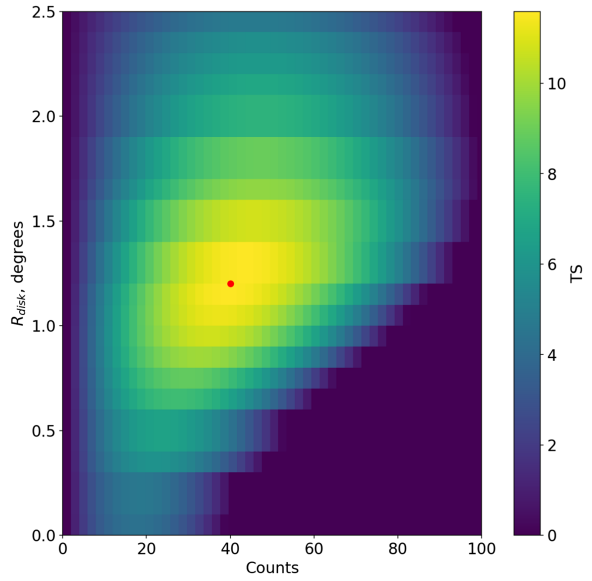

FIG. 3. Dependence of TS value on R for the disk source. Red dot shows the best-fit count number and source extension.

The functions S are tabulated over a $10° \times 10°$ region of interest.

To test the presence of the signal, we calculate the test statistic $TS(N_s) = 2(\log L(N_s) - \log L(0))$ that compares the likelihood of the presence of nonzero signal with any number of counts N_s to the likelihood of the null hypothesis of zero signal counts. Bottom panel of Fig. 2 shows the TS value map of the Cocoon region. We find a disk (Gaussian) source with $TS = 11.6$ (10.8) for the extension $R = 1.2°$ (0.7°), at the position of $RA = 208.3° \pm 0.9°$, $\mathrm{Dec} = 40.9° \pm 0.9°$ provides the best fit to the data. The red dot and circle in the bottom panel of Fig. 2 show the best-fit source position and its uncertainty. Figure 3 shows the dependence of the TS value on R. One can see that only a mild excess of $N_s < 20$ events is seen for $R = 0$. This is consistent with the analysis of the point source at the nearby position of 2HWC J2031 + 415 in which an excess of 13 events is found [15].

Given the limited statistics of the neutrino data we perform the spectral analysis fixing the spectral slope to $\Gamma = -3$ consistent with LHAASO KM2A measurement. To convert the physical source flux in the neutrino count number, we use the instrument response functions of IceCube [17]. We calculate the expected energy distribution of detectable neutrinos in narrow energy intervals dE_{ν_μ} by multiplying the neutrino spectrum $dN_{\nu_\mu}/dE_{\nu_\mu}$ by the neutrino effective area $A_{\nu_\mu}(E_{\nu_\mu})$ and exposure time T_{exp} that we find summing all time intervals in the "uptime" tables provided with the data release [17]. We calculate the expected muon energy distribution by convolving the neutrino energy distribution with the "smearing matrices" that provide the probability density functions to find muon events with given reconstructed muon energy E_μ, angular reconstruction precision σ, and misalignment with respect to the reference neutrino arrival direction θ for given neutrino energy E_{ν_μ} and declination Dec. To find the flux normalization, we fit the muon counts in each energy bin using likelihood defined through the W-statistic (we use implementation from the GAMMAPY package [25,26]). The flux normalization found in the aperture photometry analysis is $F_0 = 3.3^{+2.0}_{-1.0} \times 10^{-11}/(\mathrm{TeV\ cm^2\ s})$. In the likelihood analysis we estimate the flux uncertainty as an interval of TS values larger than $TS_d - 4.5$, given that we adjust disk size R along with N_s [27]. This gives $F_0 = 3.3^{+2.1}_{-2.3} \times 10^{-11}/(\mathrm{TeV\ cm^2\ s})$ consistent with the result of the aperture photometry analysis. The red solid line and red error band in Fig. 1 show the estimate of the disk source flux from the likelihood analysis. We show the all-flavor neutrino flux that is directly comparable to the γ-ray flux within the hadronic models. We assume the full mixing of the neutrino flavors.

III. DISCUSSION AND CONCLUSIONS

We searched for the extended neutrino excess in the direction of the Cygnus region in the publicly available 10 yr IceCube neutrino telescope dataset. We have found an excess of events from the direction of Cygnus Cocoon inconsistent with a background fluctuation at $\simeq 3\sigma$ confidence level. The neutrino flux from the source is found to be comparable to the flux of γ rays in the multi-TeV energy range seen by HAWC and LHAASO.

Our analysis confirms the hypothesis that the emission from the Cygnus Cocoon region is powered by interactions of cosmic-ray protons and atomic nuclei. It reveals evidence for a Galactic high-energy neutrino source on the sky. Low statistics of the neutrino data does not allow us to see if there is a compact (or even pointlike) neutrino source at the location of either PSR J2032 + 4127, detected by HAWC and LHAASO (HAWC J2031 + 415 or LHAASO J2032 + 4130) or at Cyg X-3 that has been considered as candidate neutrino source based on γ-ray data [28,29]. The complex morphology of the extended multimessenger source may be influenced not only by the location of possible point(s) of injection of cosmic rays, but also by the effect of anisotropic diffusion of cosmic rays preferentially spreading along the direction of the ordered Galactic magnetic field, which is almost aligned along the line of sight in the Cygnus direction [30,31]. Better constraints on the properties of the neutrino source will be possible with the increase of the neutrino signal statistics provided by the new km^3 class neutrino telescopes KM3NET [32] and IceCube-Gen2 [33].

[1] M. Kachelrieß and D. V. Semikoz, Prog. Part. Nucl. Phys. **109**, 103710 (2019).
[2] R. Abbasi *et al.* (IceCube Collaboration), Science **380**, adc9818 (2023).
[3] A. Neronov and D. Semikoz, Astropart. Phys. **72**, 32 (2016).
[4] A. Neronov and D. Semikoz, Astron. Astrophys. **633**, A94 (2020).
[5] A. Neronov, D. Semikoz, J. Aublin, M. Lamoureux, and A. Kouchner, Phys. Rev. D **108**, 103044 (2023).
[6] C. Tchernin, J. A. Aguilar, A. Neronov, and T. Montaruli, Astron. Astrophys. **560**, A67 (2013).
[7] W. Cash, P. Charles, S. Bowyer, F. Walter, G. Garmire, and G. Riegler, Astrophys. J. Lett. **238**, L71 (1980).
[8] B. Uyanıker, E. Fürst, W. Reich, B. Aschenbach, and R. Wielebinski, Astron. Astrophys. **371**, 675 (2001).
[9] M. Ackermann, M. Ajello, A. Allafort, L. Baldini, J. Ballet, G. Barbiellini, D. Bastieri, A. Belfiore, R. Bellazzini, B. Berenji *et al.*, Science **334**, 1103 (2011).
[10] HEGRA Collaboration, Astron. Astrophys. **393**, L37 (2002).
[11] A. A. Abdo, B. Allen, D. Berley, E. Blaufuss, S. Casanova, C. Chen, D. G. Coyne, R. S. Delay, B. L. Dingus, R. W. Ellsworth *et al.*, Astrophys. J. Lett. **658**, L33 (2007).
[12] ARGO-YBJ Collaboration, Astrophys. J. **790**, 152 (2014).
[13] A. U. Abeysekara, A. Albert, R. Alfaro, C. Alvarez, J. R. A. Camacho, J. C. Arteaga-Velázquez, K. P. Arunbabu, D. A. Rojas, H. A. A. Solares, V. Baghmanyan *et al.*, Nat. Astron. **5**, 465 (2021).
[14] Z. Cao *et al.* (LHAASO Collaboration), Sci. Bull. **69**, 449 (2024).
[15] M. G. Aartsen, M. Ackermann, J. Adams, J. A. Aguilar, M. Ahlers, M. Ahrens, C. Alispach, K. Andeen, T. Anderson, I. Ansseau *et al.*, Phys. Rev. Lett. **124**, 051103 (2020).
[16] S. Abdollahi, F. Acero, M. Ackermann, M. Ajello, W. B. Atwood, M. Axelsson, L. Baldini, J. Ballet, G. Barbiellini, D. Bastieri *et al.*, Astrophys. J. Suppl. Ser. **247**, 33 (2020).
[17] IceCube Collaboration, arXiv:2101.09836.
[18] IceCube Collaboration, Science **376**, 538 (2022).
[19] A. Neronov, D. Savchenko, and D. V. Semikoz, Phys. Rev. Lett. **132**, 101002 (2024).
[20] J. R. Mattox, D. L. Bertsch, J. Chiang, B. L. Dingus, S. W. Digel, J. A. Esposito, J. M. Fierro, R. C. Hartman, S. D. Hunter, G. Kanbach *et al.*, Astrophys. J. **461**, 396 (1996).
[21] R. Abbasi, Y. Abdou, T. Abu-Zayyad, J. Adams, J. A. Aguilar, M. Ahlers, K. Andeen, J. Auffenberg, X. Bai, M. Baker *et al.*, Phys. Rev. D **83**, 012001 (2011).
[22] M. G. Aartsen, M. Ackermann, J. Adams, J. A. Aguilar, M. Ahlers, M. Ahrens, C. Alispach, K. Andeen, T. Anderson, I. Ansseau *et al.*, Astrophys. J. **886**, 12 (2019).
[23] IceCube, Fermi-LAT, MAGIC, AGILE Team, HAWC, HESS, and VERITAS Collaborations, Science **361**, eaat1378 (2018).
[24] IceCube Collaboration, Science **361**, 147 (2018).
[25] C. Deil, R. Zanin, J. Lefaucheur, C. Boisson, B. Khelifi, R. Terrier, M. Wood, L. Mohrmann, N. Chakraborty, J. Watson *et al.*, in *Proceedings of the 35th International Cosmic Ray Conference (ICRC2017)*, Vol. 301 of International Cosmic Ray Conference (Proceedings of Science, Trieste, Italy, 2017), p. 766.
[26] C. Nigro, C. Deil, R. Zanin, T. Hassan, J. King, J. E. Ruiz, L. Saha, R. Terrier, K. Brügge, M. Nöthe *et al.*, Astron. Astrophys. **625**, A10 (2019).
[27] W. S. S., Ann. Math. Stat. **9**, 60 (1938).
[28] V. S. Berezinskii, C. Castagnoli, and P. Galeotti, Astrophys. J. **301**, 235 (1986).
[29] N. Sahakyan, G. Piano, and M. Tavani, Astrophys. J. **780**, 29 (2014).
[30] R. Jansson and G. R. Farrar, Astrophys. J. **757**, 14 (2012).
[31] G. Giacinti, M. Kachelrieß, and D. V. Semikoz, J. Cosmol. Astropart. Phys. 07 (2018) 051.
[32] KM3NeT Collaboration, Astropart. Phys. **111**, 100 (2019).
[33] M. G. Aartsen, R. Abbasi, M. Ackermann, J. Adams, J. A. Aguilar, M. Ahlers, M. Ahrens, C. Alispach, P. Allison, N. M. Amin *et al.*, J. Phys. G Nucl. Phys. **48**, 060501 (2021).